

**DEVELOPMENT OF A COMPUTED RADIOGRAPHY-BASED  
WELD DEFECT DETECTION AND CLASSIFICATION SYSTEM**

**WILLIAM KOAY FONG THAI**

**UNIVERSITI SAINS MALAYSIA**

**2008**

**DEVELOPMENT OF A COMPUTED RADIOGRAPHY-BASED  
WELD DEFECT DETECTION AND CLASSIFICATION SYSTEM**

**by**

**WILLIAM KOAY FONG THAI**

**Thesis submitted in fulfilment of the  
requirements for the degree of  
Master of Science**

**JANUARY 2008**

## **ACKNOWLEDGEMENTS**

I would like to express my heartfelt gratitude to my supervisor, Associate Professor Dr. Lim Chee Peng for his supports and motivations. His guidance and incisive advice have inspired me to generate fruitful approaches in achieving the objective in this research. Without his effort, I would not able to bring this research to a completion.

My gratitude is extended to my beloved family members especially my nieces, Ying, Yen, Yue and Jun that support and encourage me all along without hesitation. I treasure dearly their encouragement and moral support.

Last but not least, I would like to express my sincere gratitude to my friends, Ooi Woi Seng who has dedicated his time to guide me in image analysis, Lim Say Yarn in programming, Wang Shir Li in analyzing the codes, Ng Theam Foo in printing support, and all my friends, for their unlimited support and encouragement.

## **TABLE OF CONTENTS**

Acknowledgements	ii
Table of Contents	iii
List of Tables	vi
List of Figures	vii
List of Abbreviations	xi
Abstrak	xiii
Abstract	xiv

### **CHAPTER 1 - INTRODUCTION**

1.1	Background of Research	1
1.2	An Overview of Weld Defect Detection and Classification	5
1.3	Problem Statement	7
1.4	Research Objectives	9
1.5	Research Scope and Approach	10
1.6	Thesis Outline	11

### **CHAPTER 2 - A LITERATURE REVIEW ON WELD DEFECT DETECTION AND CLASSIFICATION**

2.1	Introduction	13
2.2	An Overview of Computed Radiography in Non-Destructive Testing (NDT) Applications	13
2.3	Weld Defect Detection and Classification System	15
2.3.1	Weld Extraction and Segmentation	16
2.3.2	Defect Detection	18
2.3.3	Feature Extraction and Defect Classification	25
2.4	Artificial Neural Networks	30
2.5	Adaptive Resonance Theory	32
2.5.1	Architecture of ART	34
2.5.2	Pattern Matching Cycle in ART	35
2.5.3	The Unsupervised Fuzzy ART Network	38
2.5.4	The Supervised Fuzzy ARTMAP Network	44
2.6	Summary	50

### **CHAPTER 3 – WELD DEFECT SEGMENTATION USING ADAPTIVE THRESHOLDING**

3.1	Introduction	52
-----	--------------	----

3.2	Background Study	52
3.3	Collection of Computed Radiography Images	54
3.4	Pre-processing of Weld Radiograph Images	59
3.4.1	Component Detection, Extraction and Alignment	60
3.5	Segmentation of Weld Radiograph Images	62
3.5.1	Adaptive Thresholding	63
3.6	The Niblack Approach	65
3.6.1	Defect Segmentation with the Niblack Approach	66
3.6.2	Results and Discussion	69
3.7	Summary	69

## **CHAPTER 4 – WELD DEFECT PROFILING USING A FLAW MAP APPROACH**

4.1	Introduction	71
4.2	Background	71
4.3	The Flaw Map	73
4.3.1	Generating the Flaw Map	75
4.3.2	Cleansing the Flaw Map	77
4.3.3	Joining Line Segments by Region Growing	79
4.3.4	Detecting the Defects with Adaptive Thresholding	81
4.4	Difference Between the Flaw Maps of Line-shaped Defects and Circular Defects	88
4.5	Summary	90

## **CHAPTER 5 – FEATURE EXTRACTION OF WELD DEFECTS FROM THE FLAW MAPS**

5.1	Introduction	92
5.2	Shape Descriptor	92
5.2.1	Sub-Regions in Weld ROI	95
5.2.1.1	Segmentation of the Sub-Regions	95
5.3	Texture Information	99
5.4	Feature Extraction from The Flaw Map	102
5.5	Summary	109

## **CHAPTER 6 – WELD DEFECT CLASSIFICATION USING NEURAL-NETWORK-BASED SYSTEMS**

6.1	Introduction	110
-----	--------------	-----

6.2	Combining Predictions from Multiple FAM Networks	110
2.6.1	Majority Voting	111
2.6.2	Multi-Agent Systems	111
2.6.2.1	A Multi-Agent Classifier System (MACS)	112
6.3	Experimental Setup	115
6.4	Results and Discussion	118
6.4.1	Multi-defect Classification	120
6.4.2	Comparison between Single-defect and Multi-defect Classifications	122
6.4.3	Overall Performance	123
6.4.4	Factors Contributing to Classification Errors	124
6.5	Summary	125
<b>CHAPTER 7 – CONCLUSIONS AND FUTURE WORK</b>		
7.1	Conclusions and Contributions	126
7.2	Suggestions for Future Work	129
<b>REFERENCES</b>		132
<b>APPENDIX</b>		
A	Experiments Details of Chapter 6	140
<b>PUBLICATION LIST</b>		147

## LIST OF TABLES

		Page
Table 2.1	Function and Input channels of each layer	35
Table 3.1	Typical weld defects in computed radiographs	56
Table 3.2	Database of collect defect images in this study	58
Table 3.3	(a) Results of the Niblack approach on the ROI of <i>Connector Weld</i> (b) Results of the Niblack approach on the ROI of <i>Cover Weld</i>	67
Table 4.1	The flaw table is obtained from the sample image presented in Figure 4.9	85
Table 4.2	Summary of flaws extracted from flaw maps of both line-shaped and circular defects	91
Table 5.1	Description of Shape Descriptors	94
Table 5.2	(a) The corresponding sub-region features for flaws in Figure 5.5(d) (b) The extracted features for flaws in Figure 5.5(d) using shape and texture descriptors	104
Table 5.3	(a) The corresponding sub-region features for flaws in Figure 5.8(c) (b) The corresponding features for flaws in Figure 5.8(c)	106
Table 6.1	Classifier systems used for experimentation	116
Table 6.2	The extracted flaws used for experimentation	117
Table 6.3	Classification results of circular defect	118
Table 6.4	Classification results of line-shaped defect	119
Table 6.5	Results of multi-defect classification	121
Table 6.6	Comparison of single defect and multi-defect classification results	122
Table 6.7	Summary of the overall classification accuracy rates	123

## LIST OF FIGURES

		Page
Figure 1.1	Development of weld radiograph in radiography systems (Hayes, 1998).	3
Figure 2.1	A generic architecture of an unsupervised ART network. The two major subsystems are the attentional subsystem and orienting subsystem. $F_1$ and $F_2$ represent two layers of nodes in the attentional subsystems. Nodes on each layer are fully interconnected to the nodes on each layer. A plus sign (+) indicates an excitatory connection, whereas a negative sign (–) indicates an inhibitory connection	34
Figure 2.2	<p>A schematic diagram of a typical pattern matching in an ART network.</p> <p>(a) An input vector, <math>\mathbf{a}</math>, goes to <math>F_1</math> and generates a STM pattern <math>X</math> at <math>F_1</math>. Output pattern <math>X</math>, <math>U</math> then is transmitted to <math>F_2</math> via the bottom-up LTM traces.</p> <p>(b) A winning node in <math>F_2</math> is selected based on the highest response. A prototype with pattern <math>P</math> is sent to <math>F_1</math> via top-down LTM traces.</p> <p>(c) In response to a mismatch between the input vector, <math>\mathbf{a}</math>, and then new <math>F_2</math> STM pattern <math>X^*</math>, a reset signal is initiated to inhibit the winning node. The hypothesis testing cycle is repeated by re-applied the input vector, <math>\mathbf{a}</math> to <math>F_1</math>.</p>	37
Figure 2.3	The Fuzzy ART Architecture	39
Figure 2.4	The architecture of Fuzzy ARTMAP	46
Figure 3.1	two weld ROIs are to be extracted for each fuel nozzle, i.e. left and right side, for each weld program, (a) <i>Connector Weld</i> and (b) <i>Cover Weld</i>	55
Figure 3.2	Each side of weld ROIs is divided into four areas, i.e. background of radiograph, weld and non-weld regions, and heat-affected zones	56
Figure 3.3	The summary of weld image pre-process methodology	59
Figure 3.4	Red-squared portion in the image is used for automatic alignment of the component	61



Figure 3.5	(a) The binary and skeleton process (b) Calculation of slant component degree	61
Figure 3.6	A graphical representation of adaptive thresholding	64
Figure 4.1	The weld ROI is extracted from the original image	75
Figure 4.2	The weld ROI are scanned line by line as shown by the gray vertical lines with their corresponding line profiles plotted. Black and gray crossed-points represent peaks and troughs, respectively	76
Figure 4.3	The flaw-map of the weld ROI with $L_I$ after being scanned line by line. Gray circle indicates the location of defect $L_I$	76
Figure 4.4	Removing unwanted area in non-weld regions based on location points and edges between black and white regions	78
Figure 4.5	Comparison of the flaw-maps before and after cleansing	79
Figure 4.6	The operation of region growing	80
Figure 4.7	The effect of brightness decrement on the line profile (a) The line profile of a non-defect line segment (gray circle) is plotted (b) The line profile at a brightness value of 396 (c) The line profile at a brightness value of 296 turns into a straight	81
Figure 4.8	The effect of contrast and brightness decrement on the flaw map (a) The original flaw map is obtained from the original brightness values of 396 and contrast value set at 600. The flaw map generated after (b) the contrast is reduced to 0; and (c) the brightness is reduced to 96	82
Figure 4.9	The contrast and brightness values of the weld ROI are decreased and a flaw map is generated for each level of decrement (a) The flaw-maps of contrast decrement; (b) The flaw-maps of brightness decrement	84
Figure 4.10	Three line segments are detected from the contrast and brightness adjustment operations. However, these line segments, i.e. the flaws in the flaw map above represent possible defects or non-defects in weld ROI image	86

Figure 4.11	The operation of extracting windowed images with reference to the respective flaws mapped to their locations in weld ROI image	87
Figure 4.12	(a) Original weld ROI image, (b) The resultant flaw map after contrast and brightness adjustment produces 20 line segments, (c) The result of Niblack thresholding produces 8 line segments. The gray circle indicates the defect of <i>LOF</i>	88
Figure 4.13	Two flaw maps are generated based on the characteristics of the defects	89
Figure 5.1	(a) The original weld ROI image of a component (b) The proposed sub-regions	96
Figure 5.2	The process of obtaining sub-regions from a <i>Connector Weld</i> component	97
Figure 5.3	The process of obtaining sub-regions from a <i>Cover Weld's</i> component	98
Figure 5.4	Interpreted weld ROI image of <i>Connector Weld</i>	103
Figure 5.5	The corresponding flaw map for the component in Figure 5.4	103
Figure 5.6	The graph of the normalized features from Table 5.2(b)	105
Figure 5.7	Interpreted weld ROI image of <i>Cover Weld</i>	106
Figure 5.8	The corresponding flaw map for the component in Figure 5.7	106
Figure 5.9	The graph of the normalized features from Table 5.7(b)	109
Figure 6.1	The proposed multi-agent system	114
Figure 6.2	A schematic diagram of the defect classification systems	116
Figure A1	FAM fine-tuning process for <i>Connector Weld</i> in classification of circular defect	141

Figure A2	FAM fine-tuning process for <i>Connector Weld</i> in classification of line-shaped defect	142
Figure A3	FAM fine-tuning process for <i>Connector Weld</i> in classification of multi-defect (line-shaped defect)	143
Figure A4	FAM fine-tuning process for <i>Cover Weld</i> in classification of circular defect	144
Figure A5	Figure A5 - FAM fine-tuning process for <i>Cover Weld</i> in classification of line-shaped defect	145
Figure A6	FAM fine-tuning process for <i>Cover Weld</i> in classification of multi-defect (line-shaped defect)	146

### **List of Abbreviations**

ANN	Artificial Neural Network
ART	Adaptive Resonance Theory
CR	Computed Radiography
CT	Computed Tomography
DICOM	Digital Imaging and Communications in Medicine
FAM	Fuzzy ARTMAP
FE	Feature Extraction
GLCLL	Gray Level Co-occurrence Linked List
GLCM	Grey-Level Co-occurrence Matrix
k-NN	k-nearest-neighbor
LI	Linear indication
LOF	Lack of fusion
LOP	Lack of penetration
LTM	Long Term Memory
LVQ	Learning Vector Quantization
MACS	Multi-Agent Classifier System
MAS	Multi-Agent System
MLP	Multilayer Preceptron
MRI	Magnetic Resonance Imaging
MV	Majority Voting
NDE	Non-destructive Evaluation
NDT	Non-Destructive Testing
NDT & E	Non-Destructive Testing and Evaluation
PMT	photomultiplier tube
POR	Porosity
PSL	photostimulated luminescence
RBF	Radial Basis Function Network

ROI	Region of Interest
RT	Radiography Testing
STM	Short Term Memory
UC	Undercut

**PEMBANGUNAN SISTEM PENGECAMAN DAN PENGEKELASAN  
KECACATAN KIMPALAN BERASASKAN KEPADA RADIOGRAFI TERKIRA  
ABSTRAK**

Dalam penyelidikan ini, satu sistem bersepadu yang terdiri daripada satu peta kecacatan dan satu pengelas pelbagai rangkaian neural bagi peruaian, pengesanan dan pengesanan kecacatan kimpalan telah direkabentuk dan dibangun. Keberkesanan sistem yang dicadang dinilai dengan menggunakan satu pangkalan data imej daripada muncung bahanapi pesawat sebenar. Kecacatan yang diperiksa termasuk keliangan, tanda linear, lakuran yang tidak lengkap, kurang penembusan, dan potong bawah daripada imej radiograf terkira (CR) muncung bahanapi. Suatu analisis awal menunjukkan bahawa ini adalah sukar dengan hanya menggunakan kaedah pengambangan adaptif untuk meruas dan mengesan kecacatan tersebut. Oleh yang demikian, satu pendekatan peta kecacatan untuk meruang dan mengesan kedua-dua kecacatan berupabentuk bulat (keliangan) dan garis (tanda linear, lakuran yang tidak lengkap, kurang penembusan, dan potong bawah) telah direka. Seterusnya ciri-ciri imej mengandungi penghurai bentuk dan informasi tekstur ditarik keluar daripada peta-peta kecacatan untuk mencirikan dan mewakili kecacatan tersebut. Ciri-ciri imej ini digunakan sebagai corak masukan kepada sistem-sistem berdasarkan rangkaian neural untuk mengelas kecacatan ini. Dua sistem berpelbagai pengelas yang direkabentuk berdasarkan kepada satu ensembel daripada rangkaian-rangkaian neural Fuzzy ARTMAP (FAM), iaitu (i) satu sistem pengelas berpelbagai agensi (MACS) dengan algoritma pasukan timba dan (ii) satu rangkaian mengundi dengan strategi pengundian majoriti telah diselidik. Keputusan terbaik adalah dihasilkan oleh MACS dengan purata kadar ketepatan pengelasan antara 83%-88%. Keputusan-keputusan ini menunjukkan secara positif keberkesanan pendekatan peta kecacatan dan MACS yang dicadang dalam pengesanan dan pengelasan kecacatan kimpalan.

# **DEVELOPMENT OF A COMPUTED RADIOGRAPHY-BASED WELD DEFECT DETECTION AND CLASSIFICATION SYSTEM**

## **ABSTRACT**

In this research, an integrated system consisting of a flaw map and a multiple neural network classifier for weld defect segmentation, detection, and classification is designed and developed. The effectiveness of the proposed system is evaluated using an image database of real aircraft fuel nozzles. The defects examined include porosity, linear indication, lack of fusion, lack of penetration, and undercut, from computed radiography (CR) images of the fuel nozzles. An initial analysis shows that it is difficult to use the Niblack adaptive thresholding method alone to segment and detect the defects. As such, a flaw map approach to segment and detect both circular (porosity) and line-shaped (linear indication, lack of fusion, lack of penetration, and undercut) defects is devised. Image features comprising shape descriptors and texture information are then extracted from the flaw maps to characterize and represent the defects. The image features are used as input patterns to neural-network-based systems for defect classification. Two multi-classifier systems, designed based on an ensemble of the Fuzzy ARTMAP (FAM) neural networks, are investigated, i.e., (i) a multi-agent classifier system (MACS) with the bucket brigade algorithm and (ii) a voting network with the majority voting strategy. The best results are produced by the MACS with average classification accuracy rates between 83%-88%. These outcomes positively demonstrate the effectiveness of the proposed flaw map approach and the MACS for weld defect detection and classification.

# CHAPTER 1

## INTRODUCTION

### 1.1 Background of Research

Welded components and structures are widely used in almost all industries. With the awareness of the fact that weld is the weakest link in a component, and most failures of components are related to weld and weldment performance, fabricating welded components with high quality and ensuring their performance and reliability in service is critical. In this regard, various non-destructive testing (NDT) techniques have been developed to assess the weld quality without destroying the welded components.

Non-Destructive Testing and Evaluation (NDT & E) plays a crucial role in ensuring the reliability and performance of welded components. The NDT methods are able to verify the structural integrity and compliance to the standards by examining the surface and subsurface of the welded parts as well as the surrounding base metal (Hayes,1998). These methods are required to obtain the necessary information for evaluating the welds. The advantage of these methods is that an object can be examined without destroying its structures. Non-destructive Evaluation (NDE) can be conveniently applied for ensuring that the weldments are fit for the purpose. NDE places due emphasis on characterization of microstructures, residual stresses, as well as quantitative determination of size, shape, and location of a defect or anomaly. As such, evaluation of structural integrity of a welded component is ensured (Baldev *et al.*, 2000).



The technology of NDT of welds has evolved rapidly during the past few years. The methods normally used to examine the welds in NDT are visual, radiographic, ultrasonic, magnetic, penetrant, and electrical methods (Halmshaw, 1996). Among the various NDT techniques, radiography testing (RT) is often adopted in many industries to assess the weld quality by evaluating the radiographs of the welded components by a skilled inspector. RT has the capability of exposing internal defects in testing a wide variety of materials ranging from light elements such as aluminium, beryllium, magnesium, to steel, nickel, and other heavy elements (Baldev *et al.*, 2000).

In RT, a gamma-ray or X-ray beam is transmitted from the radiation source. The gamma-ray or X-ray penetrates through the welded part. Different level of absorption takes place in the defective part and the surrounding metal, depending upon the material used (Ditchburn *et al.*, 1996). A photographic record of the transmitted energy, which is called a radiograph, is produced based on different degrees of penetration of the radiant energy in the welded part, as shown in Figure 1.1. When less absorption happens owing to the thin section of the metal, dark regions occur in the radiograph where more penetration of the rays takes place. This phenomenon normally happens in the weld which has voids, such as porosity and cavities. On the other hand, thicker areas or higher density material absorb more radiation, and their corresponding areas on the radiograph are lighter such as metal inclusion in the weld. The film is developed and treated with chemical components in a darkroom before the

radiograph of the weld interior can be inspected clearly using an illumination box (Bryant *et al.*, 1989).

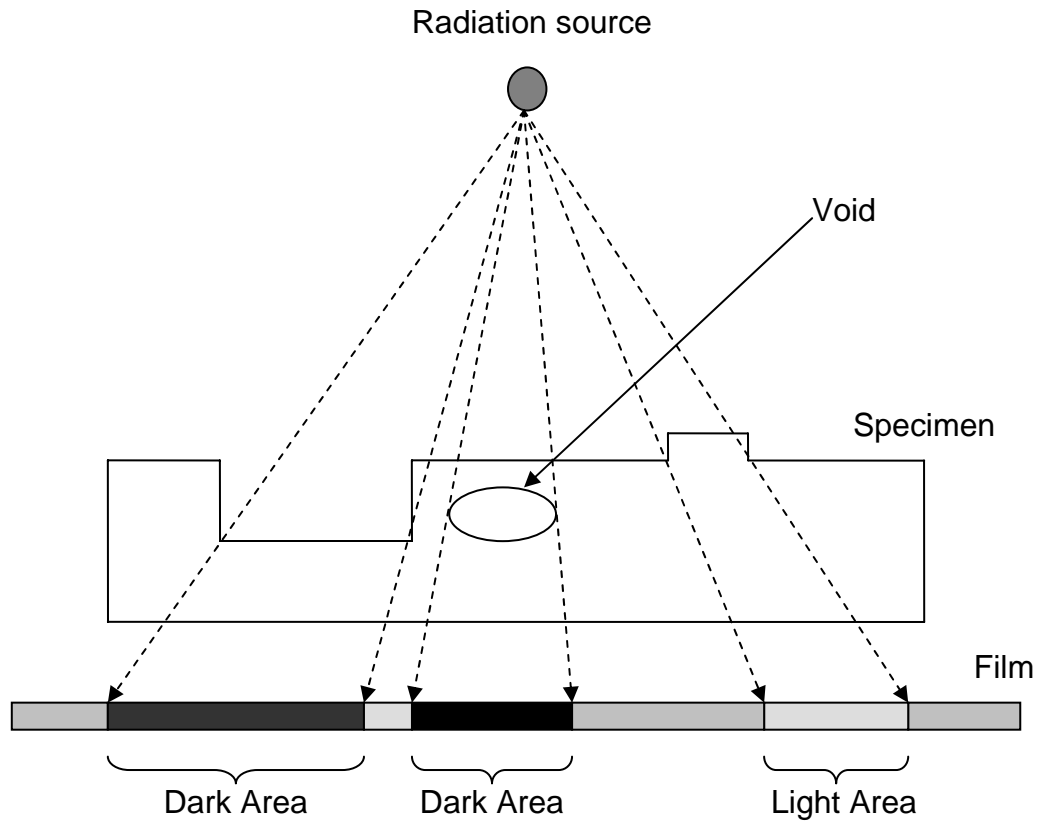


Figure 1.1 – Development of weld radiograph in radiography systems (Hayes, 1998).

The development of Computed Radiography (CR) has improved the conventional RT to a filmless testing method. CR uses very similar equipment as those of conventional RT. An imaging plate is used in place of a film to create the weld radiograph. The imaging plate contains photostimulable storage phosphors, which store the radiation level received at each point in local electron energies (Rowland, 2002). When the plate is put through the scanner, a scanning laser beam causes the electrons to relax to lower energy levels, emitting light that is measured to compute the digital image. Imaging plates can

be re-used by exposing the plate to a room-level fluorescent light to erase the image inside. The imaging plate is run through a computer scanner to read and digitize the image (Deprins, 2004). The image can then be viewed and enhanced using software that has functions very similar to those of the conventional image-processing software, such as contrast, brightness, and zoom.

In both RT and CR methods, the produced radiography is inspected by a trained NDT inspector. A decision is then made on the acceptability of the component or object under test. As such, the NDT interpreter must have a thorough understanding on the weld process and the associated flaws as well as the acceptance criteria as specified in the reference codes and standards (Liao and Ni, 1996).

Since the evaluation of radiographs by human inspectors remains subjective and inconsistent, computer-aided systems for automatic interpretation of radiographs have attracted a lot of research interest. The main function of computer-aided systems is to detect defective areas in the internal parts of a weld and to classify the defects accordingly with less human involvement. In the following sections, a brief overview of automatic defect detection methods of weld radiograph is presented. Next, the main problems of the existing methods in defect detection of weld radiographs are explained. Then, the research objectives and research scopes are defined. This is followed by a discussion on the research approach adopted. The thesis outline is presented at the end of the chapter.

## 1.2 An Overview of Weld Defect Detection and Classification

In general, weld radiographs are inspected by a trained inspector using visual acuity. The interpretation of the radiograph is very much depends on the knowledge and experience of the inspector. Human interpretation of radiograph is a difficult and tedious task especially when there are a large number of defects to be checked. Moreover, different interpreter may have different opinion on a given radiograph (Nockeman *et al.*, 1991). Even the same interpreter sometimes may have a different opinion at different time (Kaftandjian *et al.*, 1998). As such, the interpretation result is pretty subjective and uncertain (Fucsok and Schaimach, 2000).

Use of an automated interpretation software is more reliable as its decision is not dependent on subjective factors, such as tiredness after a long period of interpretation. Therefore, the development of automated interpretation systems for weld radiograph inspection grows rapidly over the past decade. With the advancement of computing power and digital image processing, automated interpretation systems with functions of film digitization, image pre-processing, weld area localization, defect segmentation detection, and defect classification are made possible (Khalid *et al.*, 2000).

In digitization, the weld radiographs are digitized using image capturing devices such as a scanner or a camera with an illumination box beneath. The captured image is then loaded into a computer. The digitization process converts the information from a weld radiograph into a digital format with

different levels of gray values. Some of the defects such as incomplete penetration and porosity normally appear darker than the background in the digitized weld image (Hayes, 1998). Other defects, such as metal inclusion, appear brighter as compared with the background.

On the other hand, Morro *et al.* (2004) has described the use of CR technology as a direct replacement for radiographic film. The digitization process is not required as images can be obtained directly in computer image format. Using the information obtained from the images, further processing is carried out to improve the image quality such as contrast enhancement, noise elimination and shading correction (Nacereddine *et al.*, 2004). Therefore, the CR technology with an automated interpretation system makes the inspection process faster and more reliable.

In defect detection and classification, weld defects that exist in the digitized image need to be identified. Normally, a number of features such as area, compactness, length, breadth, elongation, mean pixels, and central moment are quantitatively measured, and they are classified according to their types (Feher, 2001). This classification stage often involves feature extraction and a detailed pattern analysis routine. Currently, artificial intelligence methods such as artificial neural network (ANN) and fuzzy system have been actively used in the decision making of weld defect classification tasks (Lashkia, 2001; Wang and Liao, 2002; Silva *et al.*, 2004).

### 1.3 Problem Statement

In general, automatic defect interpretation of weld radiographs consists of five stages, i.e., image digitization, pre-processing, weld extraction, defect segmentation, and defect classification (Khalid *et al.*, 2000). However, digitized radiographic images are often corrupted by non-uniform illumination, contain noise, and have low contrast levels (Lashkia, 2001). These undesirable factors caused the research of automated defect detection of weld radiograph to focus on pre-processing and defect segmentation and to improve the image quality so that a better visibility of the defects on the image can be produced. The interpretation of weld quality, however, is still carried out manually by referring to the processed image.

The development of CR has brought X-ray imaging to a new era of digital filming as well as inspection. The NDT interpreter no longer needs to place the radiographic film on a illuminator and vary the intensity of the light source. The inspection is done by viewing the computed radiograph in a computer monitor and using an imaging software to adjust the contrast and darkness levels to expose the defects. More defects can be exposed using the features in the imaging software such as image enlargement, cropping, enhancement, measurement, etc. Nevertheless, the required knowledge and experience of NDT interpreters is regardless of digitized or computed radiographs.

As such, much research has been conducted to further automate the interpretation of weld radiographs by developing automated defect detection and classification systems (Khalid *et al.*, 2000; Sofia and Redouane, 2002;

Nacereddine and Tridi, 2005). Although work related to automate defect detection from digitized radiographs has been carried out, the detection and classification of multiple defects from a single image has not been addressed widely. Besides that, these areas of work are mainly based on digitized radiographs, and not on CR images.

From the literature review, there is a lack of past research regarding the investigation of suitable characterization features for each defect type. In other words, the features which have been used in the classification process are not subjected to a detail investigation of their suitability to identify certain defect types (Bonser and Lawson, 1998; Wang and Liao, 2002; Mery and Berti, 2003) or small defects (Mery *et al.*, 2002; Sun *et al.*, 2005). Besides that, the intensity plot of the weld in the digitized images (Wang and Liao, 2002; Mery and Berti, 2003) normally are treated as a Gaussian curve, which may not be the case in a lot of radiographs. Both the limitations lead the classification system to yield lower classification accuracy rates that are yet to achieve the optimal outputs in weld defect detection and classification.

Classification of weld defect types is an important issue. This is because the defect detection process alone is not sufficient to assess the weld quality automatically. As a result, a skilled NDT inspector is needed to interpret the radiograph. Furthermore, the occurrences and statistics of different defect types reflect different problems in the welding process. If root causes of different defect types can be identified in the early stage, then the process can be halted before more defects are produced. However, not much work has

been done in the past in discriminating different types of weld defects. Recently, several authors (Aoki and Suga, 1999, Wang and Liao, 2002) have shown interest in classifying defects using artificial neural network (ANN). However, most of the work focuses on the Multi-Layer Perceptron model, and other ANN models are not studied. Furthermore, a single ANN model may not be able to overcome the problem of detecting multiple defects in radiographs.

This research undertakes a detailed study of the existing techniques and algorithms used in image processing of CR. More importantly, by emulating the interpretation process of the NDT inspector, a defect detection and classification system that can segment the defects from weld images with non-Gaussian intensity profile automatically and classify the multiple defects from a single CR image into different categories has been designed and developed. In addition, the defect classification system is developed based on the combined predictions from a multi-classifier model devised using the ANN technology.

#### **1.4 Research Objectives**

The main aim of this research is to design and develop an automatic defect detection and classification system that is able to detect and classify multiple defects in CR images. The specific research objectives are as follows.

- (a) To collect a set of real CR images and generate a database of weld ROI images for analysis using image processing techniques.
- (b) To investigate the use of gray level thresholding to process the whole weld radiographs and to develop defect segmentation using adaptive thresholding from the ROI images.



- (c) To develop a flaw map approach for detecting weld defects from the ROI images
- (d) To identify shape descriptors and texture features to characterize and represent the weld defects
- (e) To develop a semi-automatic defect classification system based on a neural-network-based multi-classifier system to detect and classify the weld defects

### **1.5 Research Scope and Approach**

This research is focused on the development of an automated defect detection and classification system which consists of image pre-processing, weld extraction, defect segmentation, and defect classification. The weld radiographs used in developing the classification system consists of real fuel nozzles CR images collected from an aerospace servicing company. The weld defects investigated include porosity, linear indication, lack of fusion, lack of penetration, and undercut. The entire defect detection and classification system is developed in MATLAB 7.0.4.

The images used in this research comprise real CR images of fuel nozzle components from an aerospace service company. First, the weld ROI image is aligned and extracted from the whole image using gray level thresholding. The extracted ROI image is then segmented using background subtraction and adaptive thresholding. This step, which serves as an initial attempt to detect weld defects in CR images, is necessary so that effort can be focused on

processing and analysing weld regions, and not on the non-weld regions. The Niblack thresholding method along with background subtraction are studied

As explained in the problem statement, there is a lack of work in emulating the interpretation process of the NDT inspector in examining the weld defects while taking the advantages of CR technology. In order to extract relevant features from the image database, a review of the flaw map approach (Liao and Li, 1998) is conducted, and a revised flaw map is developed to emulate the interpretation process of the NDT inspector. Then, shape and texture descriptors are extracted to define the flaws. Unlike most published work that focuses on the Multilayer Preceptron (MLP) neural network, the Fuzzy ARTMAP (FAM) neural network is studied in this research for defect classification. The classification system is first developed based on a single FAM, and the efficiency is assessed using features extracted from the flaw map. Then, a multi-agent classifier based on a pool of FAM networks combined with the bucket brigade algorithm is applied for defect classification. The classification accuracy rates are analysed, discussed, and compared with those from a pool of FAM networks combined by using the majority voting strategy.

## **1.6 Thesis Outline**

This thesis is arranged in accordance with the objectives as mentioned in Section 1.4. Chapter 2 reviews various automated weld defect detection and classification methods. A thorough discussion on the advantages and limitations of the existing approaches for automated defect detection and classification is provided. In Chapter 3, a weld extraction methodology based

on gray level thresholding is firstly developed to extract the weld part from the whole CR image. This is followed by the weld defect segmentation process using the Niblack adaptive thresholding technique.

Chapter 4 discusses the flaw map approach to extract weld defect from the Region of Interest (ROI) images. Chapter 5 describes the features used to characterize the segments extracted from the flaw map. Chapter 6 details the development of a multi-agent classifier system using a pool of FAM neural networks, whereby the predictions from multiple FAM networks are combined by using the bucket brigade algorithm. Conclusions and suggestions for further work related to this research are drawn and presented in Chapter 7.

## **CHAPTER 2**

### **A LITERATURE REVIEW ON WELD DEFECT DETECTION AND CLASSIFICATION**

#### **2.1 Introduction**

In this chapter, a review of computed radiography (CR) in non-destructive testing (NDT) applications is presented. Besides, recent research work related to weld defect detection and classification is surveyed. The survey focuses on three important components, i.e., defect segmentation, defect detection, and defect classification.

#### **2.2 An Overview of Computed Radiography in Non-Destructive Testing (NDT) Applications**

Non-Destructive Testing and Evaluation (NDT&E) of welded components plays a crucial role in ensuring reliable performance of welded components (Baldev *et al.*, 2000). NDT methods such as radiography, ultrasonic, magnetic particle, liquid penetrant, eddy current are required to obtain necessary information in the weldments whereas NDE emphasized on the evaluation of structural integrity of welds such as characterization of microstructures, shape and location of a defect or anomaly (Baldev *et al.*, 2000). The primary advantage of NDT methods is that the object can be examined without destroying it. Today, the options for radiographic testing (RT) include not only film, but with recent technological advantages, digital solutions that are reliable and cost effective, such as Computed Radiography (CR) are possible to be

implemented in NDT inspection applications. More and more applications can be covered by the improving image quality of digital radiography systems (Deprins, 2004).

In this research, the investigation is focused on CR images. In CR, an imaging plate (IP) containing the storage phosphor is positioned in a light-tight enclosure, exposed to the x-ray image and then read out by raster scanning with a laser to release the photostimulated luminescence (PSL). This results in the emission of shorter wavelength (blue) light in an amount proportional to the original x-ray irradiation. The blue PSL light is collected with a light guide and detected with a photomultiplier tube (PMT). The PMT signal is digitized to form the image on a point-by-point basis (Fujita *et al.*, 1989). X-ray absorption mechanisms are identical to those of conventional phosphor screens used with film. They differ in that the useful optical signal is not derived from the light emitted in prompt response to the incident radiation, but rather from subsequent emission when the latent image, consisting of trapped charge, is optically stimulated and released from metastable traps (Rowlands, 2002). Imaging plates can be re-used for a certain periods and images can be viewed in a few minutes comparing to the exposing process of photographic films as well as saved images in storage media rather than keeping films in achieved box.

CR images usually are saved in DICOM (Digital Imaging and Communications in Medicine) format as set by the CR system, owing to the advantages as stated in DICOM standard (The DICOM standard, 2006). Nowadays, most of the created DICOM images are saved in 16 bit grayscale

format to allow better enhancement during inspection process although there are DICOM images in 8-bit and 12-bit grayscale formats.

With CR, the NDT interpreter examines radiograph image on a computer monitor using an imaging software. Visualization in CR is made easy and reliable with the availability of image enhancement, enlargement and measurement tools in the imaging software. In addition, comparing CR and film (or digitized images from films), the details of pixel information in CR images allow the NDT interpreter to expose more defects and confirm non-defects in an attempt to reduce the false alarm rate. During inspection, the NDT interpreter needs to decide the quality of weld based on individual's interpretation skills, knowledge, and experience.

### **2.3 Weld Defect Detection and Classification System**

The use of CR in NDT applications has become popular with the growth of higher computing power as well as larger storage media, such as hard disk and DVD (Deprins, 2004). However, the interpretation skills and knowledge on the digitized or CR remain the same. Human interpreters are still the decision maker of the weld quality. In the past years, both film and real-time radiography relied on human experts to perform manual interpretation of images (Liao and Li, 1998). Nowadays most inspections are still done by human experts in manufacturing plants but with the assistance of more advanced software tools, particularly image processing to enhance, enlarge the ROI in radiograph with the objective of exposing defects. Although manual interpretation is a cost effective method, the assessment of radiographic films by human interpreters is

sometime difficult and subjective when a great number of films are to be interpreted (Kaftandjian *et al.*, 1998). A survey conducted by volunteers in laboratories from Croatia, Hungary and Poland regarding the NDT reliability of routine radiographic film evaluation by human inspectors showed that experience and education play significant roles in the evaluation of radiographs (Fucsok and Scharmach, 2000).

### **2.3.1 Weld Extraction and Segmentation**

Weld extraction is usually the first step in the development of defect detection and classification systems for weld radiographs. A weld region may have several appearances in a radiograph depending on the joint types used, such as butt joint, T-joint, corner joint, lap joint and edge joint (Bryant *et. al.*, 1989). The discontinuities in weld are normally subjected to various types of defects owing to the improper welding techniques. Lawson and Parker (1994) described an intelligent system for segmenting defects for quality evaluation, where the inspection of welded structures normally focuses within the weld area. Hence, extraction of welded components from the whole radiographs is an important step to reduce processing time and the false alarm of flaws which appear outside the weld region and ROI.

There have been studies on the development of algorithms to extract welds and to identify anomalies in the weld regions. Lawson and Parker (1994) developed a weld segmentation algorithm with back propagation MLP neural network as the first stage of defect detection in the weld. In Kaftandjian *et al.* (1998), background subtraction and histogram threshold were performed to

segment the defects from the background. However, false alarm happened owing to the small background regions and noise beside the actual defects. A real-time automatic detection system of weld defects was established by Sun *et al.* (2005). The minimum size of defects was 0.4 mm but the weld size of the defects was very large. When the above technology was adopted to detect the smaller defects in complex structures, false detection could happen.

In Mery and Filbert (2002), an automated flaw detection method in aluminum castings based on the tracking of potential defects in a radiosopic image sequence was presented. Special filtering and masking were used to segment the casting defects, and the casting defects in aluminum wheels were extracted by using the software PXV 5000. In addition, the defects detection algorithm could eliminate the false detection rates without discriminating the real flaws based on the multiple view geometry. However, the above researches were mainly done to detect relative larger defects. So, there are some limitations when using the methods to detect the small defects in complex structures, and this is the focus of this research.

Liao and Ni (1996) proposed a weld extraction method based on the observation of the intensity plot where the plot of a weld appeared more like Gaussian curve than the other objects in the image. The algorithms basically consisted of various steps including dividing image into sub-images, detecting peak and trough as well as similarity computation, slopes calculation and maximum weld finding in line extraction. The methodology was found to have 100% accuracy with 25 images used. Liao and Tang (1997) applied the



multilayer perceptron (MLP) neural network to extract and represent welds. Four features were extracted from Gaussian intensity plot, i.e., peak position, width, mean square error between the object and its Gaussian intensity plot, and the peak intensity. The methods of using the characteristics of Gaussian profile to extract weld region (Liao and Ni, 1996, Liao and Tang, 1997, Liao *et al.*, 2000) have a major drawback, that is, the method is only limited to weld image which has similar intensity line profile to the Gaussian bell shaped profile. For other variation of intensity profiles which is non-Gaussian line profile, the methodology will not work. Furthermore, most weld radiographs have different shapes for the intensity line profile owing to the image quality. As such, in this research, an effective weld extraction method based on the intensity line profile or gray level line profile of the image is proposed.

### **2.3.2 Defect Detection**

Much effort has been made to automate the process of defect segmentation and detection with the assistance of digital image processing techniques. Segmentation of weld defects is the most crucial part in defect detection to ensure defects do not 'escape' from the segmented image. In addition, radiographic images often contain noise. Inappropriate techniques may lead to the escape of defects. Extensive work has been carried out by a lot of researchers using various techniques and approaches, as reviewed in the following section.

With the advancement of artificial intelligence, several researchers used artificial neural network (ANN) in defect segmentation. Liao *et al.* (1999)

presented a flaw detection methodology, based on fuzzy clustering methods, to process the weld image line by line. By fitting the curve using B-spline, gray level profiles were plotted with the aim to smoothen the noise level. For each line, 25 features were extracted from the above mentioned profile. Two fuzzy systems were compared, namely fuzzy k-nearest neighbour (k-NN) algorithm which assigned class membership to sample a vector and, Fuzzy c-means algorithm that considered all the samples in the universe belonging to a certain class but with different membership. The algorithms were tested on 18 weld segments taken from 9 different weld images. It was found that the the fuzzy k-NN classifier outperformed the fuzzy c-means algorithm with the best results of 6.01% missing rate and 18.68% false alarm rate. The proposed method, however, assumed a defect-free profile to have a symmetrical appearance, which was similar to the assumption that the profile is approximately Gaussian. This limitation is the same as in the work by Liao and Ni (1996), Liao and Tang (1997) and Liao *et al.* (2000).

A segmentation method was developed by Lawson and Parker (1994) using the backpropagation network. The network was trained based on a set of image segmented by Kehoe's (Kehoe and Parker, 1992) adaptive thresholding method. To train the network, an NxN window was specified and moved across the image in a raster fashion as the input and the desired output is referred to the pixel in the thresholded image. A total of 50,000 random sets of windows were chosen to train the network. The investigation found that the window size must be larger than 9x9 to ensure convergence. The output of image was then

binarized using simple rules. The approach outperformed the original Kehoe's method, where the latter had the tendency to produce false signals.

Lashkia (2001) proposed a detection algorithm based on fuzzy reasoning to detect low contrast defects using local image characteristics, such as spatial contrast, spatial variance and distance between two contrast regions. The proposed method evaluated the object fuzzy membership value for each pixel, and pixels with high membership were detected as defects regions. A region growing method was used to extract the position and shape of defects. The reliability test was based on 117 weld radiographs with typical defects, e.g. longitudinal and transverse cracks, lack of fusion, incomplete penetration, blow hole and slag inclusions. Visual evaluation by interpreter yielded 181 defects whereas the algorithm successfully detected 177 defects. However, 35 misinterpretations occurred owing to the recognition of small noise regions. In addition, some small defects which were located near the dark boundaries would not be detected. Thus, the method was sensitive to noise in images as well as in detecting small defects near the dark boundaries.

Background subtraction methods have been used a lot in defect segmentation. In background subtraction, the background image is first estimated from the original image (Russ, 1999). This estimated background is then subtracted from the original image to obtain a resultant image which has high illumination gradient of defect. This technique is effective in segmenting image with non-uniform illumination. Daum *et al.* (1987) estimated background function using spline approximation. According to them, defect indications in

the image could be characterized by high spatial frequencies while normal welding bead and its surrounding caused gradual gray level changes with low spatial frequencies. However, the algorithm developed was found to be difficult in detecting small defect sizes. Hyatt *et al.* (1996) proposed a segmentation technique using the multi-scale method where the defects were segmented from background image to remove the background while preserving the defective area.

Besides that, Aoki and Suga (1997) presented a background estimation methodology using the “special point connecting method”. In this method, low brightness areas in the distribution were supplemented where the alleys or gaps within the brightness distribution of horizontal profile were filled up. The image was then subtracted with this estimated background.

Bonser and Lawson (1998) combined two 5X5 filter masks to detect different appearance of weld defects, namely Laws E5S5 filter and horizontal Kirsch filter. The Laws filter was used owing to its capability to accentuate 'spot' or 'blob' type defects (such as porosities and cavities) whereas Kirsch filter was more suited to detect longitudinal defect types (such as cracks, lack of penetration and slag inclusions). The resultant image was subjected to a standard deviation operator for segmentation of suspected defect areas. The detection of false alarms was found to be low, typically with a few very small isolated groups of pixels which could be ignored owing to their small size. They concluded that filtering approach was more reliable to low contract images but less sensitive to small defects.

Adaptive thresholding is a conventional segmentation method in extracting object from the background of the image. Different from Otsu's thresholding method (1979), variable thresholds are used in which the threshold value varies over the image as a function of local image characteristics (Sonka *et al.*, 1998). For each pixel in the image, a threshold has to be calculated. If the pixel value is below the threshold, it is set to the background value. Otherwise, it assumes the foreground value. Kehoe (1990) developed an approach based on the scanning of a predefined 'window' over the image and calculated variance and gradient properties within the window. Classification was made on the center of the pixel to categorise defects or non-defects based on these window properties. In another work, Kehoe *et al.* (1989) adaptively enhanced the contrast image using the same idea of a predefined 'window' where the pixel in the center was transformed based on the variance and gradient properties in the window over the image. Window sizes between 5 and 10 were found to give good result.

Palenichka and Alekseichuk (1999) presented flaw detection in radiographic images using structure-adaptive binary segmentation. The method considered was based on local binary segmentation. A model based approach which exploited multi-scale morphological object representation was used. It allowed a quick location of local objects with different sizes. Local binarization on the greatest, medium and lowest scale yielded the weld seam, the details of weld seam, and relevant defects respectively. However, the method was limited to a certain number of defect types.

The main advantage of using adaptive thresholding is that no prior knowledge of the defect characteristics is needed, and it can be applied to any possible defects despite their sizes and shapes (Lawson and Parker, 1994). In addition, this method is less sensitive to non-uniform illumination appearance in the image as the method segments the image based on the local characteristics from the image.

Alaknanda and Kumar (2005) presented an approach to process radiographic weld images, where by the Canny operator was applied to determine the boundaries of the flaws after choosing an appropriate threshold value. The boundaries were then fixed using a morphological image processing approach, i.e. dilating few similar boundaries and eroding some irrelevant boundaries decided on the basis of pixel characteristics. Finally the defects detected by this approach were categorized according to their properties, such as porosity appeared as rounded contours having dark shadows, undercut as line broad and diffused along the edge of weld, lack of fusion as thin line along the edge of weld but might be wavy and diffuse depending upon the orientation of defect with respect to the X-ray beam, incomplete penetration as edge line in the middle of weld.

In Liao and Li (1998), a flaw detection methodology was developed based on the observation that the overall line profile of a good weld (perpendicular to the weld direction) had a bell shape with some degree of local variation. A weld flaw resulted in a disruption of the bell shape. The profile

anomalies caused by weld flaws could be classified into three categories: peak, trough, and slant-concave. These profile anomalies were peak-anomaly, trough-anomaly, and slant-concave-anomaly, respectively. With weld images from Liao and Ni (1996), the images were firstly scaled and followed by background removal based on a threshold value. The threshold value was chosen by observing the histograms of the scaled images. Once the background was removed, the line image was scaled back for the subsequent processing operations. Dark image enhancement was then applied on these images because the signal-to-noise ratios in different line images differ considerably. The line images were finally normalized to ensure its maximum gray level is maintained. The spline curve fitting algorithm was used to reduce and smooth the line profiles. The smoothness of the fitted curve was controlled by changing the smoothing factor. The line profiles were plotted in a flaw map by processing the intensity of radiograph images line by line. The anomalies above were then detected by observing their corresponded characteristics to the defects. The methodology was tested with 24 weld images which contained 75 flaws of various kinds. Five flaws, which were mainly small porosities and might be acceptable according to the codes for pressure vessels, were missed. The successful defect detection rate was 93.3%. The false alarm rate was 4.2%, which was mainly caused by the lack of fusion defects or very noisy profiles having non-Gaussian characteristics. Liao and Li's methodology were dedicated to Gaussian shape of weld profiles, and their flaw map was dedicated to a single-thresholded image.